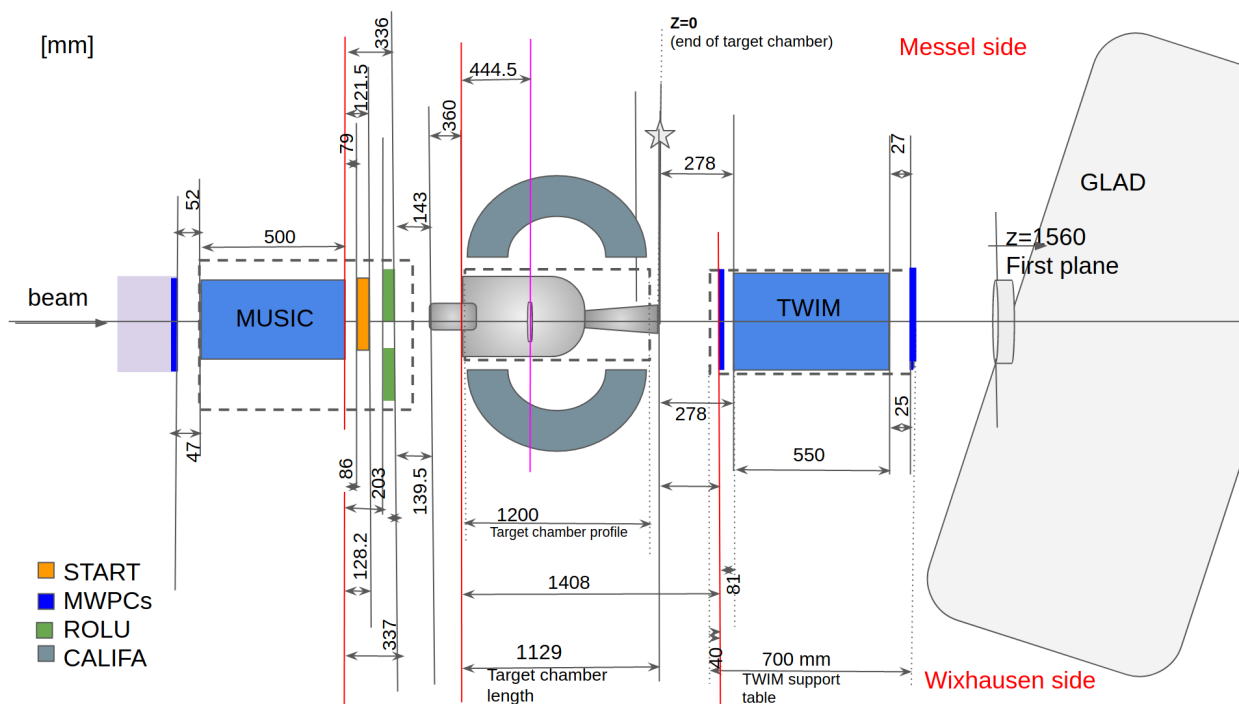
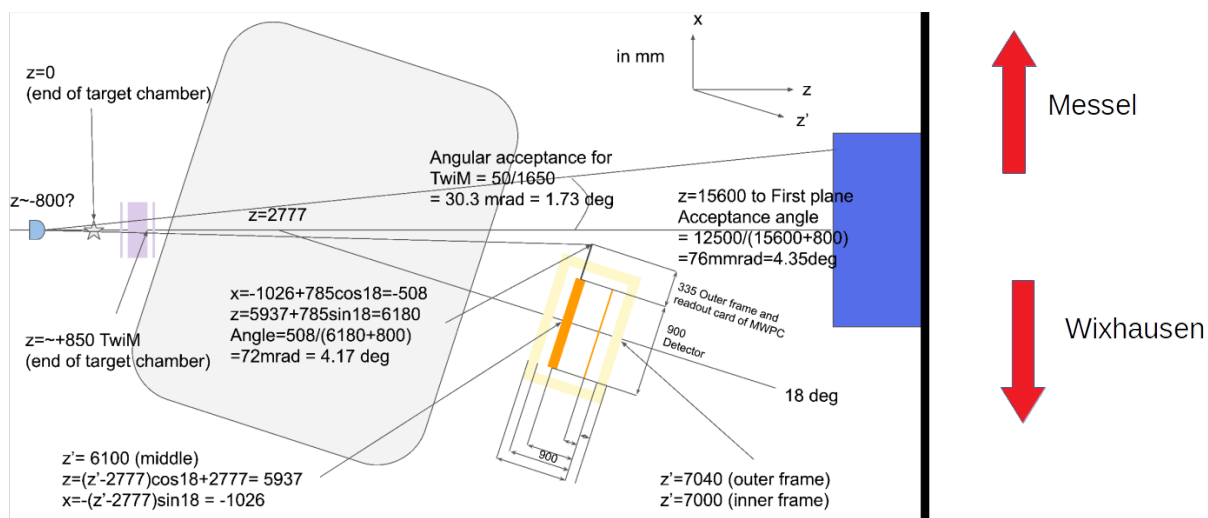


# Radius/Momentum Calculation for S444 Experiment

## February 2020 - Overview

Tobias Jenegger

## 0.1 The Setup



# 1 Geometry and relative position of the detectors in the beam direction

Here, the positions are given for the s444 and s467 experiments

z position of the MWPC0:  $z_{MW0} = -2520$  mm  
z position of the target:  $z_T = -684.5$  mm  
z position of the MWPC1 in front of the Twin-MUSIC:  $z_{M1} = 279$  mm  
z position of the middle of the Twin-MUSIC:  $z_{Twin} = 553$  mm  
z position of the MWPC2 after the Twin-MUSIC:  $z_{M2} = 854$  mm  
 $\alpha$  tilted angle of GLAD (14 degrees):  $= 0.244$  rad  
effective length of GLAD:  $L_{eff} = 2067$  mm  
z middle of GLAD  $z_{Gm} = 2577$ mm  
horizontal of the central path (18 degree)  $\theta_{out0} = \pi/10$  rad  
z position of the MWPC3 after GLAD  $z_{M3} = 5937$  mm  
z position of the ToFwall  $z_{ToFW} = 6660.2$  mm

Correspondence between the GLAD current and the magnetic field:  $I = 3584$  A,  $B = 2.2$  T

Positions of the TOFWPads:

1  $\Rightarrow$  Messel

27  $\Rightarrow$  Wixhausen

## 2 RUNS used for calibration = SWEEP RUNS without target

RUN	Beam ion	Beam Energy [AmeV]	GLAD current [A]	Comments
36	12C primary	400	1444	before broken motor, here we see that tof is about 5ns faster. So they probably changed the position of the TOFW afterwards
37	12C primary	400	1444	it has be seen that motor drive not working
38	12C primary	400	1444	tof is back with new gates *magnet sweep 1444A
39	12C primary	400	1498	
40	12C primary	400	1501	
41	12C primary	400	1501	stopped with 1558 A
42	12C primary	400	1558	
43	12C primary	400	1558	stopped with 1653 A
44	12C primary	400	1653	
45	12C primary	400	1653	stopped with 1748 A
46	12C primary	400	1748	
47	12C primary	400	1748	stopped with 1843 A
48	12C primary	400	1843	
49	12C primary	400	1843	stopped with 1938 A
51	12C primary	400	1938	
52	12C primary	400	1938	stopped with 1444 A
53	12C primary	400	1444	
54	12C primary	400	1444	stopped with 1349 A
55	12C primary	400	1349	
56	12C primary	400	1349	stopped with 1254 A
57	12C primary	400	1254	
58	12C primary	400	1254	stopped with 1159
59	12C primary	400	1159	
60	12C primary	400	1159	stopped with 1064
61	12C primary	400	1064	
62	12C primary	400	1064	stopped with 1444 A
123	12C primary	650	1748	stopped with 1957
124	12C primary	650	1957	
	=	sweeping		
	=	stable GLAD current		

### 2.0.1 Other RUNS used for various checks:

RUN 70: 2 cm C target  
 RUN 80: 10.86 mm C target  
 RUN 81: 24.53 mm CH2 target  
 RUN 67: 24 mm CH2 target  
 RUN 68: 1 cm C target  
 RUN 79: 12.29 mm CH2 target  
 RUN 75: 21.98mm C target





The curvature radius  $\rho$  is given by<sup>1</sup>:

$$\rho = \frac{L_{\text{eff}}}{2 \cdot \sin\left(\frac{\theta_{\text{in}}}{2} + \frac{\theta_{\text{out}}}{2}\right) \cdot \cos(\delta)}$$

With  $\delta$ :

$$\delta = \arctan\left(\left|\frac{\frac{\cos(\theta_{\text{out}}) - \cos(\theta_{\text{in}})}{\sin(\theta_{\text{out}}) + \sin(\theta_{\text{in}})} + \tan(\alpha)}{1 - \frac{\cos(\theta_{\text{out}}) - \cos(\theta_{\text{in}})}{\sin(\theta_{\text{out}}) + \sin(\theta_{\text{in}})} \cdot \tan(\alpha)}\right|\right)$$

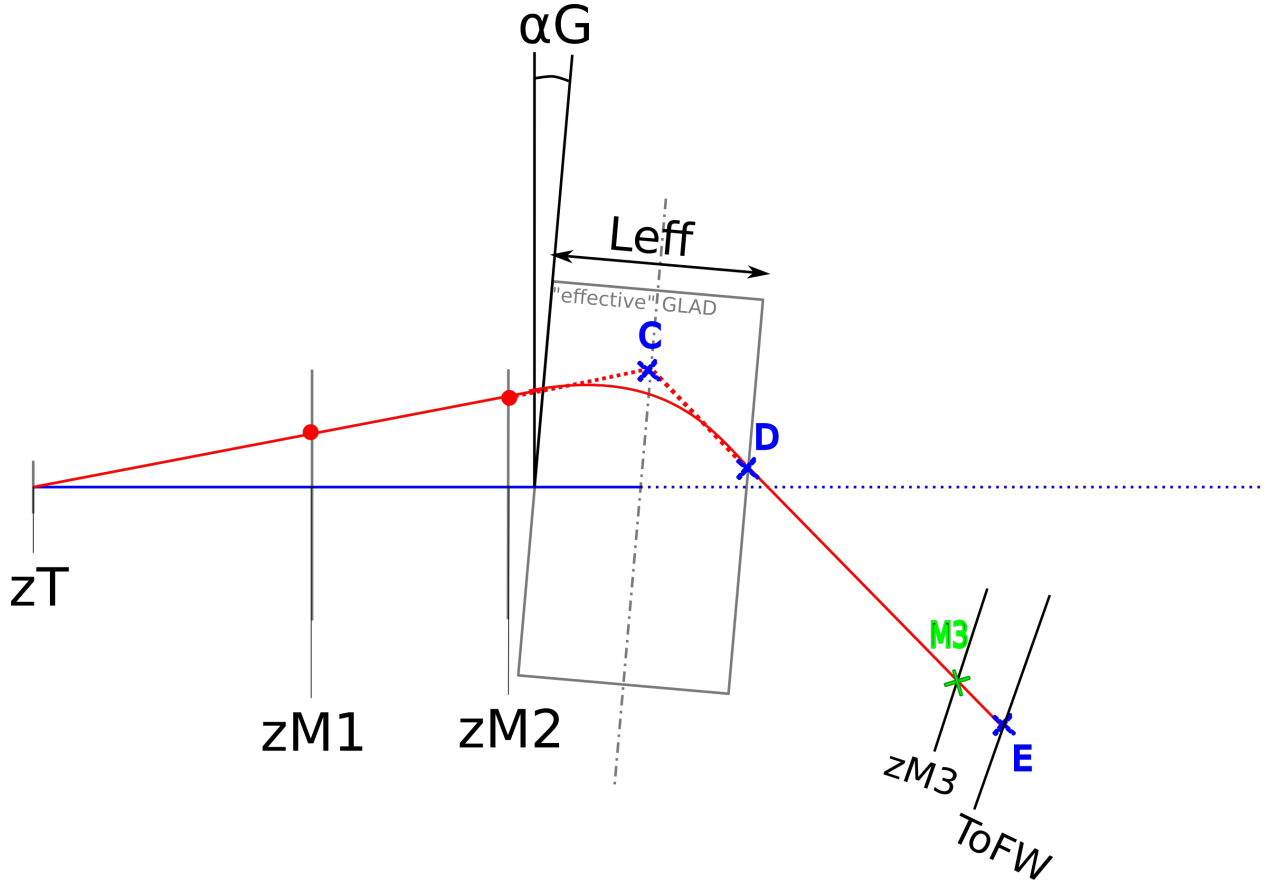
The full derivation can be found in the appendix.

The circular trajectory is then given by:

$$\omega = 2 * \left| \arcsin\left[\frac{BD}{2 \cdot \rho}\right] \right|$$

with  $BD$  = length of the  $BD$  segment

### 3.1.3 After GLAD up to the TOFW, the trajectory is a straight line



The straight line trajectory from D to E is defined by:

<sup>1</sup>for consistency checks the  $\cos(\delta)$  term can be omitted, as it plays a minor role

- ⇒ the output angle from GLAD  $\theta_{out}$
- ⇒ one absolute position after GLAD in the laboratory frame M3

With this information the straight line trajectory length after GLAD can be measured. It starts at the exit point of GLAD D and follows the straight line (characterized by the angle  $\theta_{out}$  and the absolute position at MWPC3) until the intersection with the ToFW (middle position of the ToFWall  $z_{ToFW} = 6660.2mm$ , tilted angle =  $18^\circ$ ).

Finally the pathlength in the (x,z) plane from the target position to the ToFW is given by:

$$P = AB + \rho \cdot \omega + DE$$

where:

A = (x,z) position at the target point

B = (x,z) position at the GLAD entry point

D = (x,z) position at the GLAD exit point

E = (x,z) position where the constructed trajectory line hits the ToFW

The assumption for the "Kickplane" method is that the kickpoint for each event lies on the predefined Kickplane, the symmetry axis line of the GLAD magnet.

### 3.2 The "Fit-Track" method

For the "Fit-Track" method the assumption that the kickpoint C lies on the symmetry axis line of the GLAD magnet is rejected. Instead following algorithm is applied: <sup>2</sup>

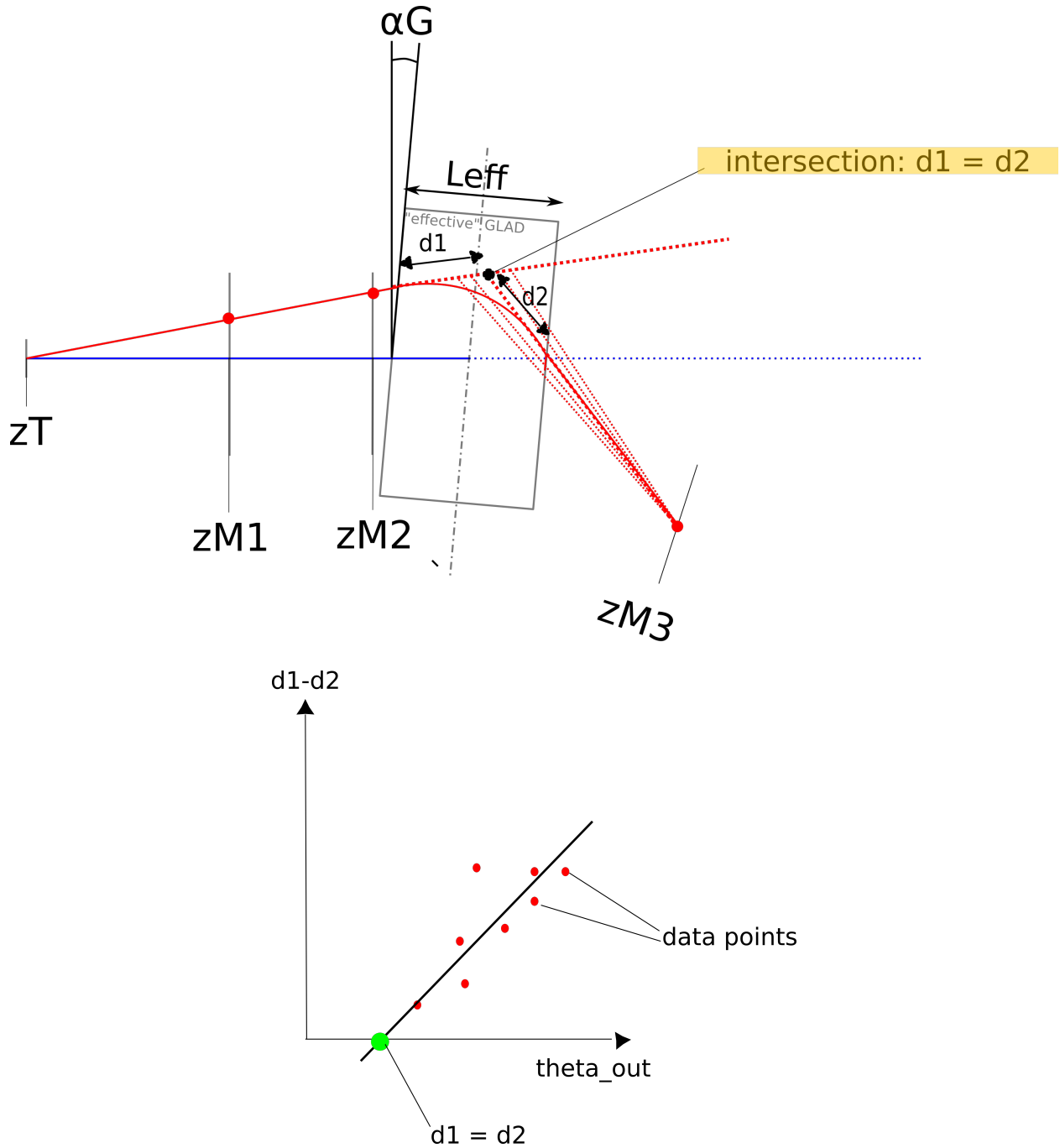
1. Extend the line of flight of the ion before the GLAD.
2. Draw a line from the point MW3 to C (as constructed with the "Kickplane" method).
3. Now sweep the straight line after the kickpoint, leaving the position MW3 unchanged but sweeping the intersection point along the inline beam.
4. For each sweeping step plot  $\theta_{out}$  versus (d1-d2) where d1 is the distance between B and the point of intersection and d2 the distance between D and the intersection point accordingly.
5. 50 sweeping steps are performed.
6. Fit the final  $\theta_{out}$  versus (d1-d2) plot with linear least square fit.

---

<sup>2</sup>This algorithm is motivated from [https://www.blogs.uni-mainz.de/fb08-kernphysik/files/2018/09/PHDThesis\\_OlgaBertini.pdf](https://www.blogs.uni-mainz.de/fb08-kernphysik/files/2018/09/PHDThesis_OlgaBertini.pdf), section 3.4



7. Find the intersection of the abscissa. The corresponding  $\theta_{out}$  value is now the corrected one which should be used for the calculation of the radius.



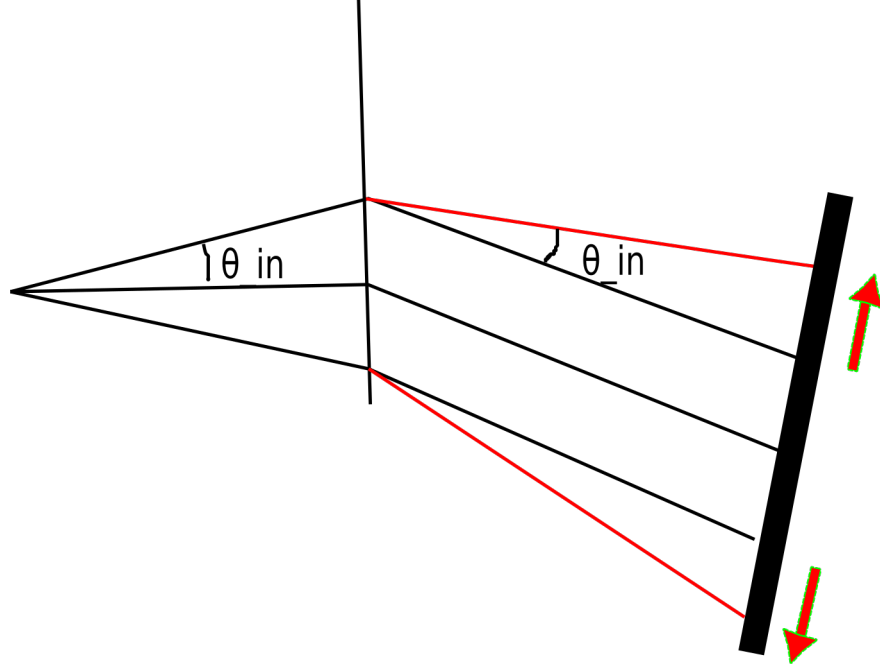
### 3.3 The "Theta\_in correction" method

Here the "Kickplane" method is used and subsequently the  $\theta_{out}$  is corrected by  $\theta_{in}$ . That means:

$\theta_{out\_corr} = \theta_{out} - \theta_{in}$ .

Consequently the  $\theta_{in}$  dependence of  $\rho$  vanishes(neglecting the  $\cos(\delta)$  term):

$$\rho = \frac{L_{eff}}{2 \cdot \sin\left(\frac{\theta_{in}}{2} + \frac{\theta_{out\_corr}}{2}\right)} = \frac{L_{eff}}{2 \cdot \sin\left(\frac{\theta_{out}}{2}\right)}$$



### 3.4 Final method: "Advanced Fit-Track" method

The same track finding algorithm as for the "Fit-Track" method is used with the only difference that the value for  $\theta_{in}$  is calculated from the fit of  $\theta_{out}$  vs.  $x_{MW3}$ :

The parameters of the linear fit are used for the calculation of  $\theta_{in}$  :

$$\theta_{in} = \alpha - a \cdot x_{MW3} - b$$

With **a** being the slope and **b** the offset of the fit. This method prevents from adding up the errors from  $\theta_{in}$  measurement.

$\alpha$  corresponds to the mean value of the  $\theta_{out}$  from the fit of  $\theta_{out}$  vs.  $x_{MW3}$ .

## 4 Plots

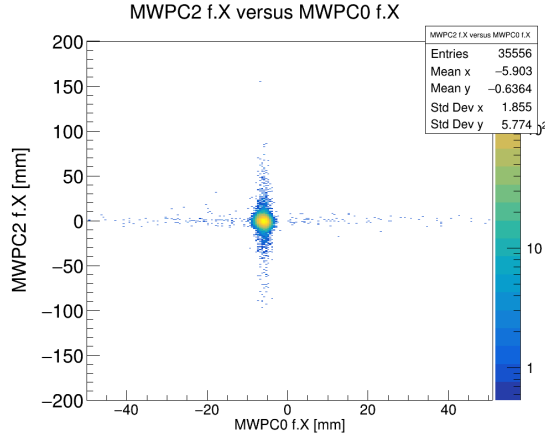
In this section all the plots for the various track finding algorithms are presented. For the calculation of the  $\theta_{in}$  angle MWPC1 and MWPC2 are used. Alternatively MWPC0 and MWPC2 could be used, to get a longer lever arm (work in progress ...).

### 4.1 MWPC1 vs MWPC2 - x position

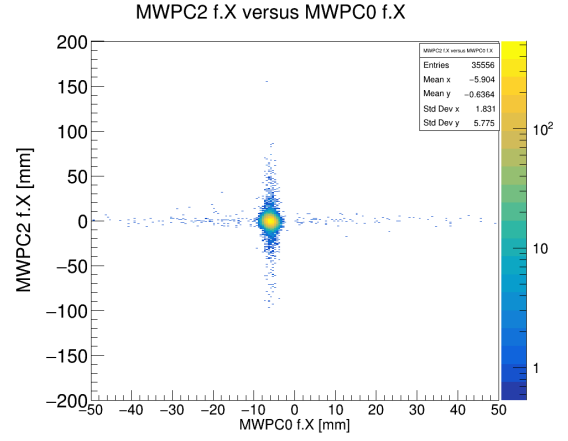


Figure 1: MWPC1 vs MPWPC2 - x position for sweep runs 39-61.

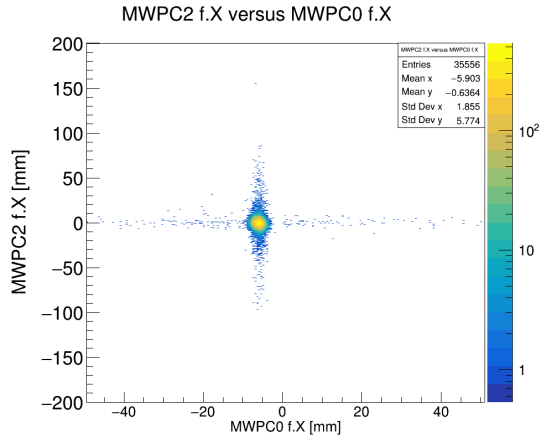
## 4.2 MW0 vs MW2- x position



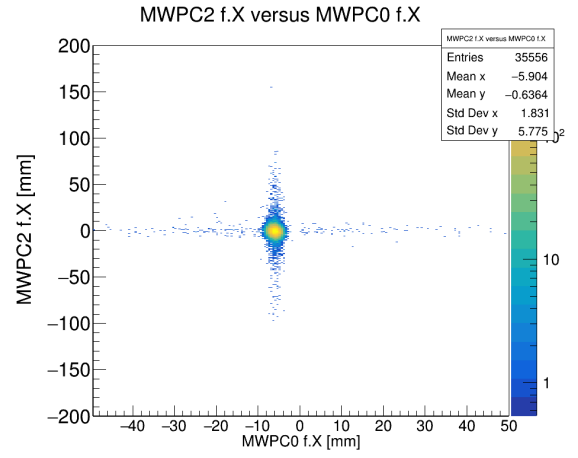
(a) "Kickplane-Method"



(b) "Theta\_in correction-Method"



(c) "Fit-Track-Method"



(d) "Advanced Fit-Track-Method"

Figure 2: MWPC2 vs MWPC0 - x position for sweep runs 39-61.

### 4.3 MW1 vs MW3 - x position

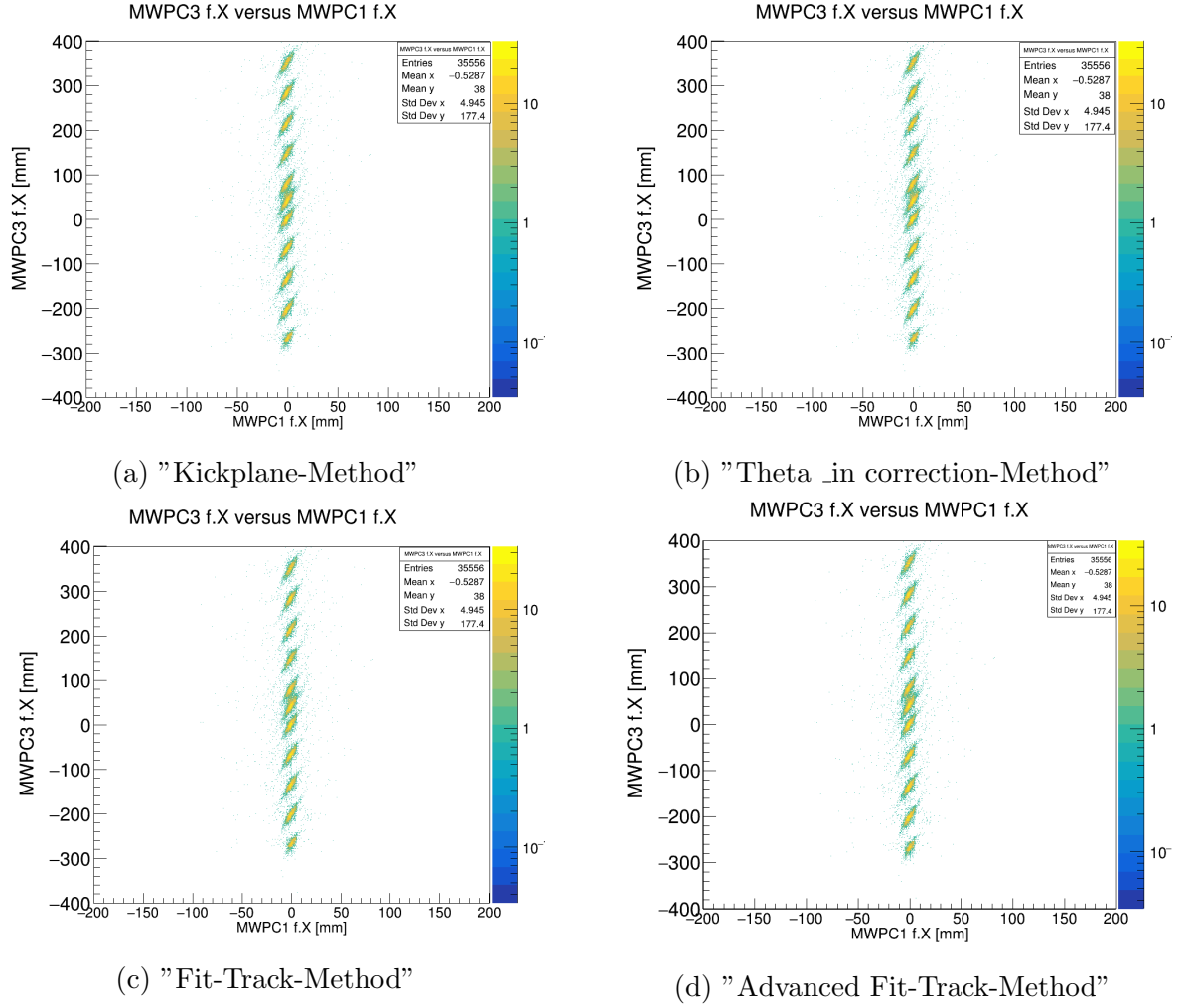
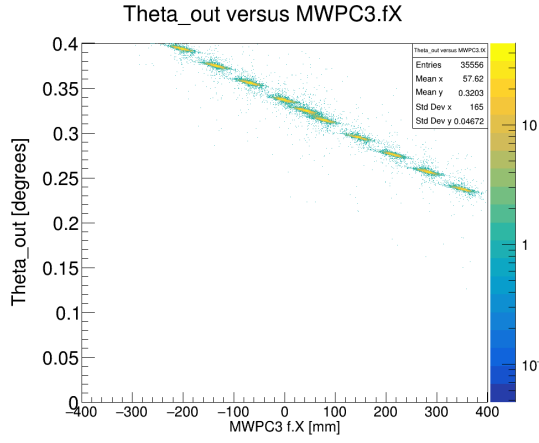
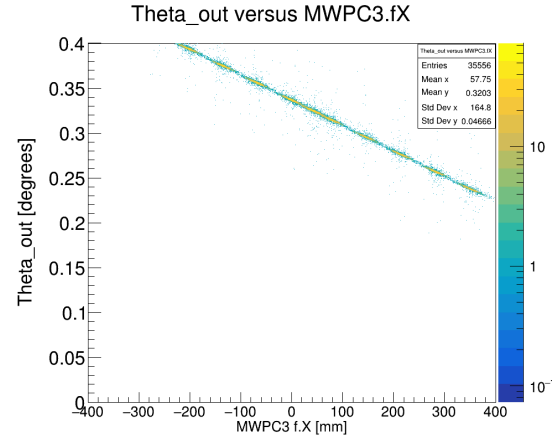


Figure 3: MWPC3 vs MWPC1 - x position for sweep runs 39-61.

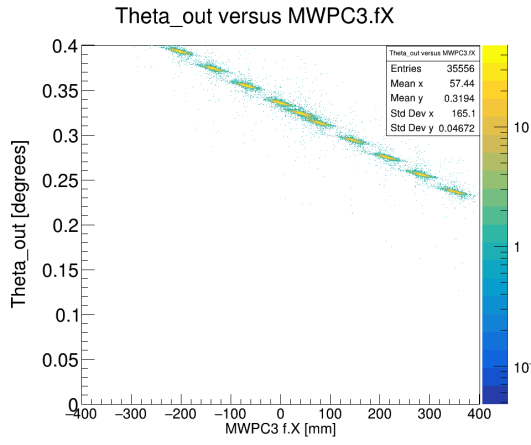
#### 4.4 theta\_out vs MW3- x position



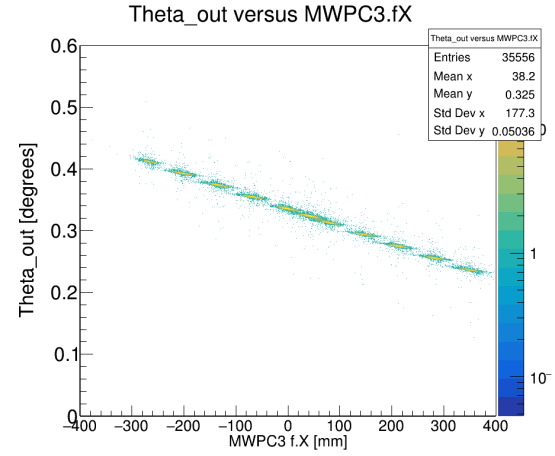
(a) "Kickplane-Method"



(b) "Theta\_in correction-Method"



(c) "Fit-Track-Method"



(d) "Advanced Fit-Track-Method"

Figure 4: Theta\_out vs MWPC3 x position for sweep runs 39-61.

## 4.5 theta\_in vs MW3 - x position

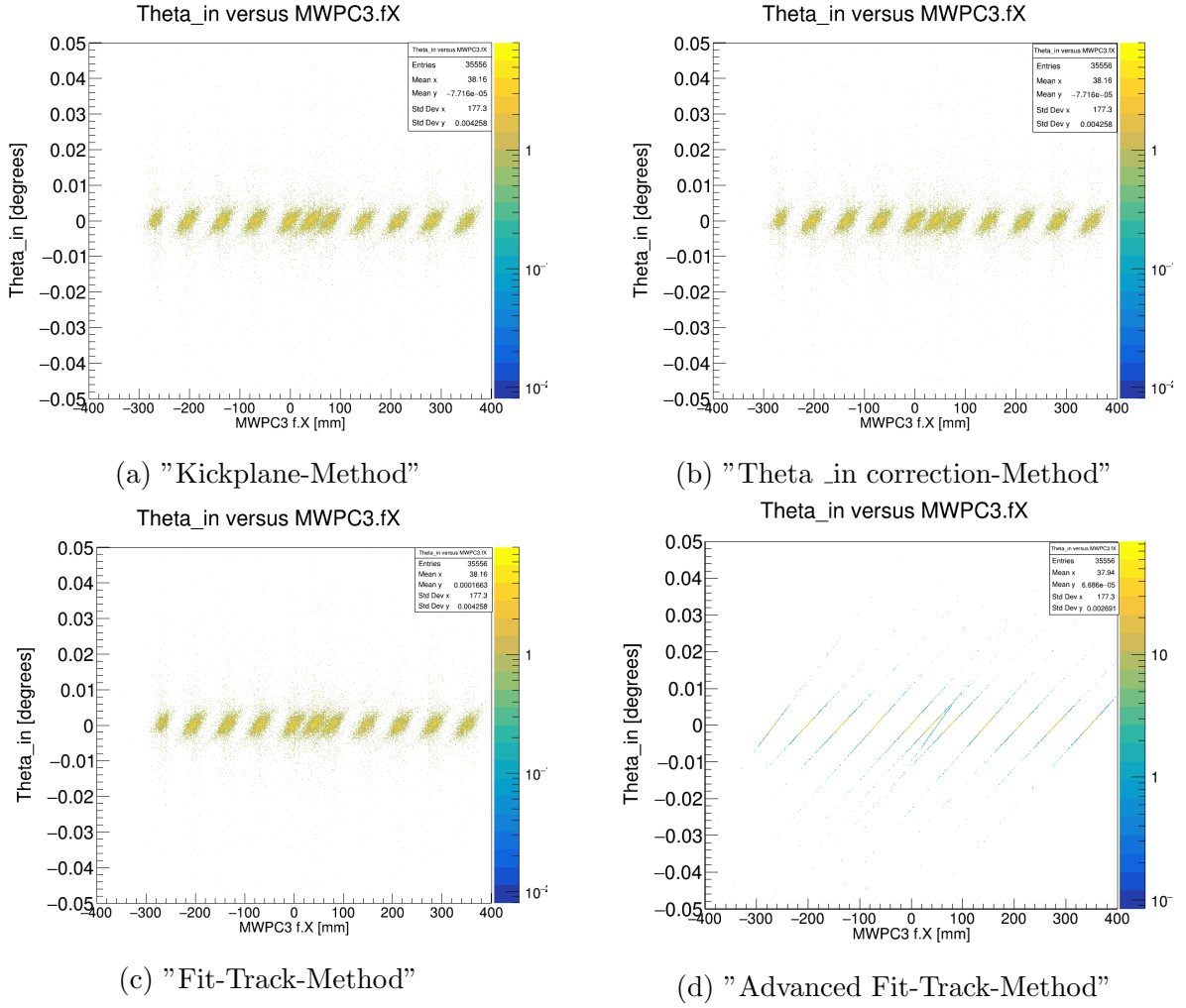


Figure 5:  $\Theta_{in}$  vs MWPC3 x position for sweep runs 39-61.

## 4.6 $\theta_{\text{out}} + \theta_{\text{in}}$ vs MW3- x position



Figure 6:  $\theta_{\text{out}} + \theta_{\text{in}}$  vs MWPC3 x position for sweep runs 39-61.



## 4.7 $\theta_{in}$ vs Radius

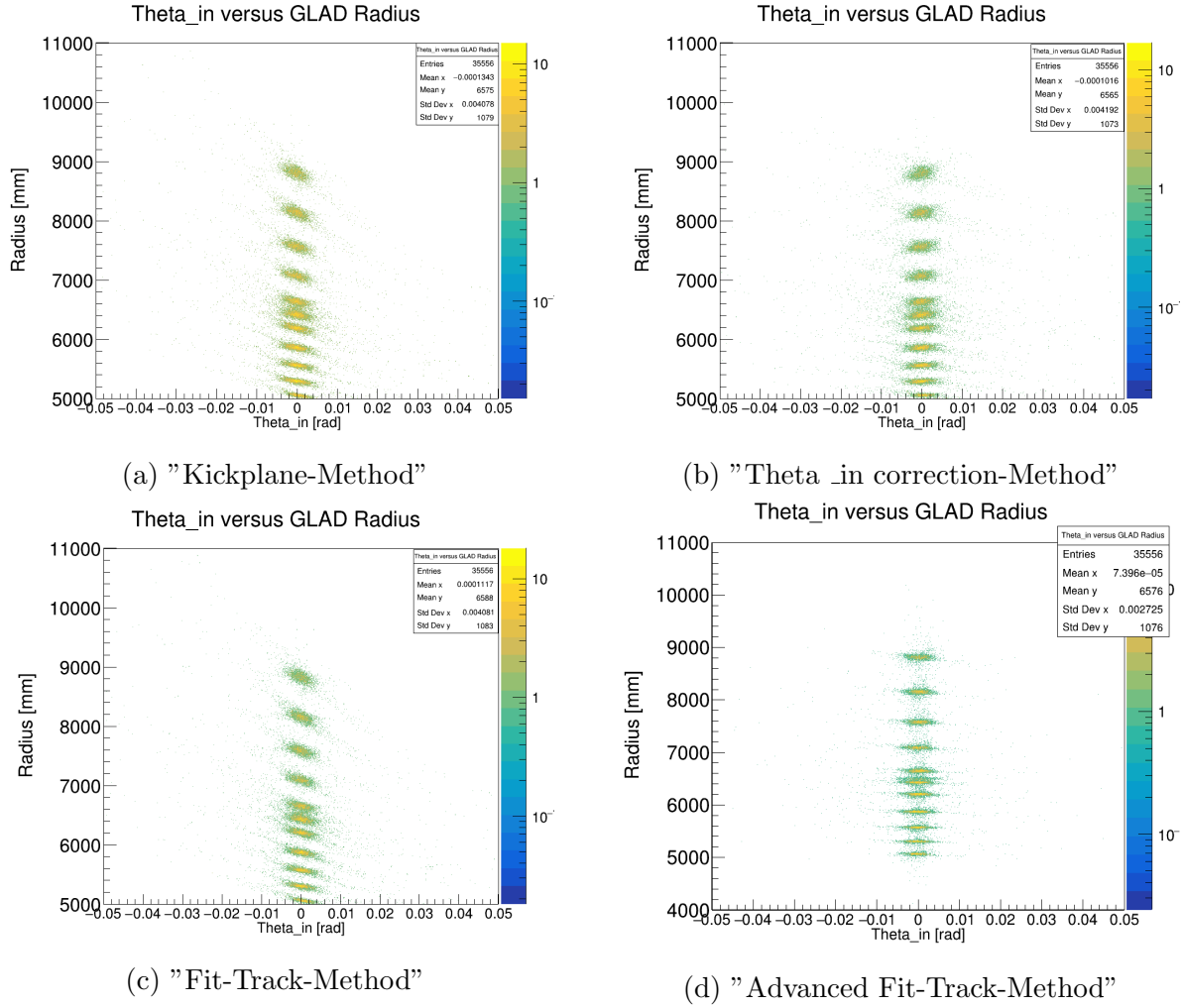


Figure 7:  $\theta_{in}$  vs GLAD Radius for sweep runs 39-61.

## 4.8 theta\_out vs Radius

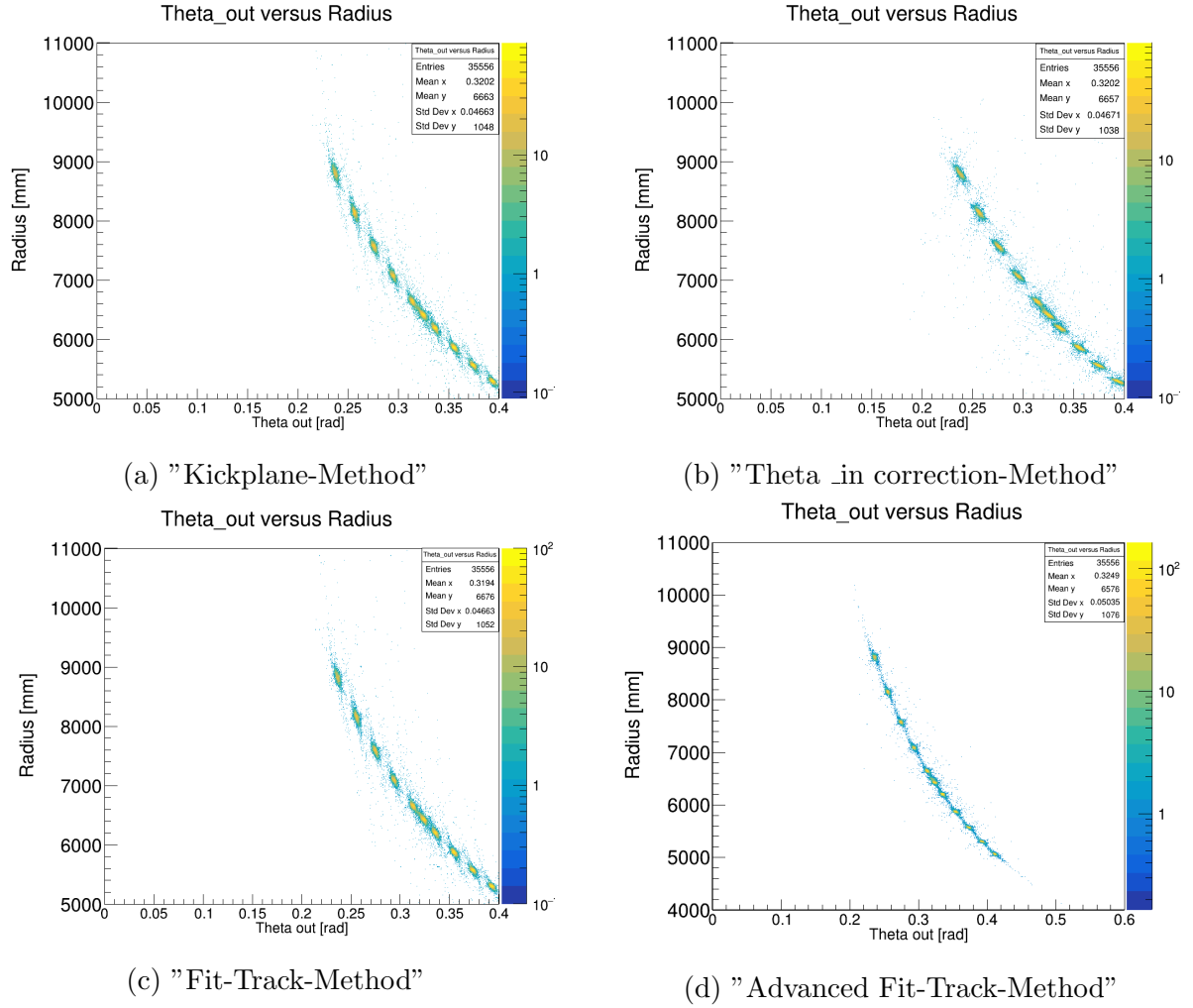
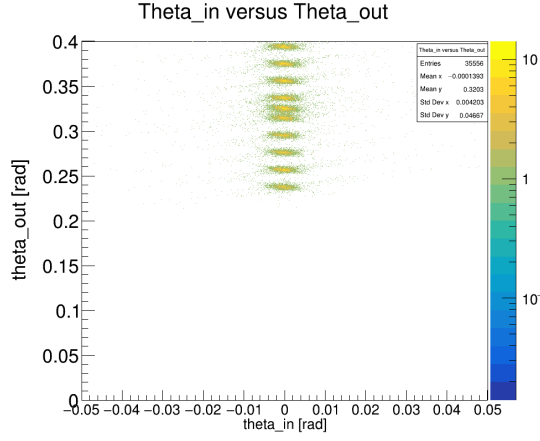


Figure 8: Theta\_out vs GLAD Radius for sweep runs 39-61.

## 4.9 $\theta_{in}$ vs $\theta_{out}$



(a) "Kickplane-Method"



(b) "Theta\_in correction-Method"



(c) "Fit-Track-Method"



(d) "Advanced Fit-Track-Method"

Figure 9:  $\theta_{in}$  vs  $\theta_{out}$  for sweep runs 39-61.

## 4.10 MW3 vs Radius - x position



Figure 10: MWPC3 x position vs GLAD Radius for sweep runs 39-61.

## 4.11 MW2 vs Radius - x position

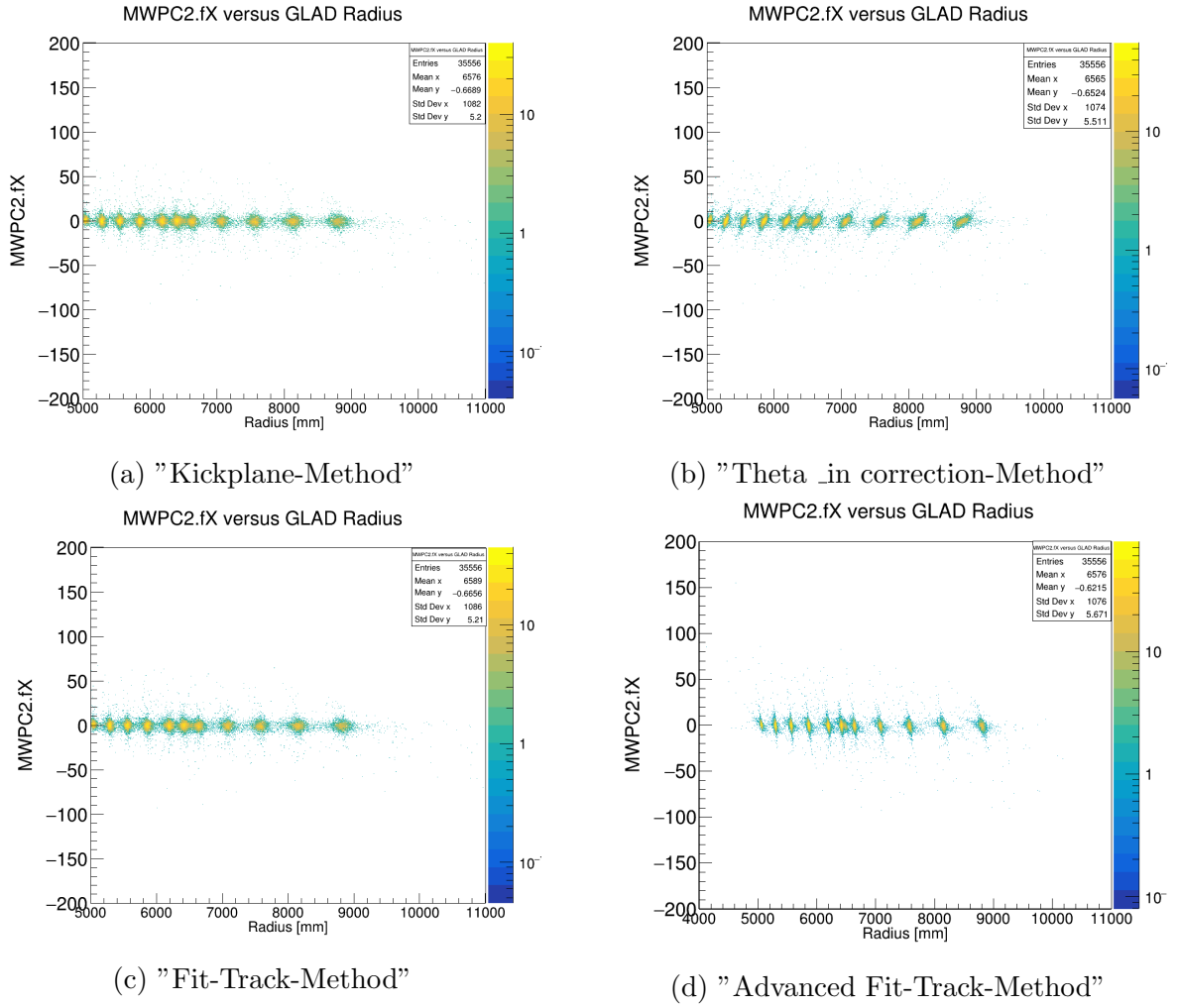


Figure 11: MWPC2 x position vs GLAD Radius for sweep runs 39-61.

## 5 Relative momentum resolution ”Advanced Fit-Track-Method”

The momentum resolution is calculated from the radius-calculation as  $\rho \sim p$ . From that follows:

$$\frac{\Delta p}{p} = \frac{\Delta \rho}{\rho}$$

For the evaluation of the resolutions for the various sweep runs the two dimensional plot ”MWPC3.fX versus GLAD Radius” is projected on the abscissa. The resulting 1D plot is fitted with a gaussian. The mean value from the fit corresponds to  $\rho$  and the  $\sigma$  to  $\Delta\rho$  respectively.

Runnr.	$\bar{\rho}$	$\sigma$	rel. resolution
39	6.48911e+03	2.13410e+01	3.289e-03
40	6.42396e+03	1.56313e+01	2.433e-03
42	6.20033e+03	1.42716e+01	2.301e-03
44	5.86854e+03	1.29449e+01	2.206e-03
46	5.57125e+03	1.31369e+01	2.358e-03
48	5.30203e+03	1.07044e+01	2.018e-03
51	5.06232e+03	1.07182e+01	2.117e-03
53	6.64556e+03	1.66141e+01	2.500e-03
55	7.08710e+03	1.91895e+01	2.708e-03
57	7.57474e+03	2.16135e+01	2.853e-03
59	8.15089e+03	2.22151e+01	2.725e-03
61	8.81055e+03	2.72038e+01	3.088e-03

With mean relative resolution  $\frac{\Delta\rho}{\rho} = 2.55\text{e-}03$ .

## 6 Limiting Radius/Momentum resolution factors

The radius/momentum resolution is limited by:

- Energy straggling
- Angular straggling
- Angular resolution of MWPC1/2
- position resolution of MWPC3 (higher order??)

## 6.1 Energy straggling

For the error calculation the mean energy inside the GLAD was used and the corresponding standard deviation. Generally for a charged particle drifting through a magnetic field the radius of the curved path the particle is following is defined as:

$$\rho = \frac{\gamma \cdot \beta \cdot m}{q \cdot B}$$

(considering  $c = 1$ )

Energy straggling has an effect on  $\beta$  and  $\gamma$  respectively. The measurement uncertainty with respect to  $\beta$  can be calculated as follows:

$$\frac{d\rho}{d\beta} = \frac{1}{(\sqrt{1-\beta^2})^3} \cdot \frac{m}{qB}$$

$$\Delta\rho_\beta = \frac{d\rho}{d\beta} \cdot \Delta\beta = \frac{\Delta\beta}{(\sqrt{1-\beta^2})^3} \cdot \frac{m}{qB}$$

with relative measurement uncertainty  $\frac{\Delta\rho_\beta}{\rho} = 5.434e - 04$

## 6.2 Angular straggling

For the error calculation originating from angular straggling it is considered only angular straggling starting from the backend of the MWPC1. That means for this error calculation it is assumed to have a perfect focussed beam undergoes no broadening until it hits the MWPC1 (always at the same x-y-z position). Angular straggling broadens the beam focus and affects therefore both  $\Theta_{in}$  and  $\Theta_{out}$ .

(angular straggling for  $\Theta_{in}$  can be neglected, higher order...)

For the calculation of measurement uncertainty with respect to  $\Theta_{out}$  we use the simplified geometrical formula of the radius:

$$\rho = \frac{L_{eff}}{2 \cdot \sin(\frac{\Theta_{in} + \Theta_{out}}{2})}^3$$

From that follows:

$$\Delta\rho_{\Theta_{out}} = -\rho \cdot \frac{1}{2 \cdot \tan(\frac{\Theta_{in} + \Theta_{out}}{2})} \cdot \Delta\Theta_{out}$$

with  $\Delta\Theta_{out} = 3.401e - 04$ . This is the value calculated with LISE++ from MWPC1 to the very center of GLAD. Hence:

$$\left| \frac{\Delta\rho_{\Theta_{out}}}{\rho} \right| = \frac{1}{2 \cdot \tan(\frac{\Theta_{in} + \Theta_{out}}{2})} \cdot \Delta\Theta_{out} = 1.079e-03$$

## 6.3 Angular resolution of MWPC1/2

$$\Delta\rho_{\Theta_{in}} = -\rho \cdot \frac{1}{2 \cdot \tan(\frac{\Theta_{in} + \Theta_{out}}{2})} \cdot \Delta\Theta_{in}$$

with  $\Delta\Theta_{in} = \frac{2 \cdot \Delta x}{L}$ <sup>4</sup> and L the (z-)distance between MWPC1 and MWPC2 (= 575mm).

---

<sup>3</sup>on the following pages I set  $\Theta_{in} = 0$  and  $\Theta_{out}$  to the value given by the GLAD field calculator(Mass = 12, Charge = 6, Energy = 400 A/MeV, Current = 1444), see <http://web-docs.gsi.de/~land/glad/>.

<sup>4</sup> $\Theta_{in} = \frac{x_2 - x_1}{L}$ ,  $\Delta\Theta_{in} = \left| \frac{d\Theta_{in}}{dx_2} \right| \cdot \Delta x_2 + \left| \frac{d\Theta_{in}}{dx_1} \right| \cdot \Delta x_1 = \frac{2 \cdot \Delta x}{L}$

With  $\Delta x = 0.1mm$  it follows:

$$\left| \frac{\Delta \rho \Theta_{in}}{\rho} \right| = 1.104e-03.$$

Adding up the above errors quadratically we get:

$$\left| \frac{\Delta \rho}{\rho} \right| = \sqrt{(5.434 \cdot 10^{-4})^2 + (1.079 \cdot 10^{-3})^2 + (1.104 \cdot 10^{-3})^2} = 1.64 \cdot 10^{-3}$$

## 6.4 Limiting Radius resolution factors on data

For this subsection RUN 53 (with GLAD current = 1444A) is taken in account.

From the table of relative radius resolution we see that for RUN 53 it corresponds to 2.500e-03. The contribution from angular resolution of MWPC1/2 is 1.104e-03 (see previous section). The major limiting factor, the angular straggling can be retrieved from the resolution of theta \_out. It has to be considered that the resolution of theta \_out is affected by the beam broadening before the MWPC1. To account for that it has to be analyzed the impact of theta \_in on theta \_out.

Therefore an offset of 1 mrad is added to theta \_in and the mean values for theta \_out can be compared :

- theta \_out without shift:  $3.13257 \cdot 10^{-1}$
- theta \_out with 1 mrad theta \_in shift:  $3.13912 \cdot 10^{-1}$
- difference:  $6.55 \cdot 10^{-1} \text{mrad}$

That means we have a translation factor (for small angles) of 0.655 for theta \_in to theta \_out.

The error calculation in the previous section predicts following angular straggling error:

$$2.5 \cdot 10^{-3} = \sqrt{(1.104 \cdot 10^{-3})^2 + \left( \left| \frac{\Delta \rho \Theta_{out}}{\rho} \right| \right)^2}$$

follows:

$$\left| \frac{\Delta \rho \Theta_{out}}{\rho} \right| = 2.24 \cdot 10^{-3}$$

$$\Rightarrow 2.24 \cdot 10^{-3} \cdot \tan(0.15625) \cdot 2 = 7.1 \cdot 10^{-4} = \Delta \theta_{out}$$

The angular resolution of theta \_out from data is 1.78045E-03. From this value the angular beam broadening (multiplied by the translation factor) before MWPC1 has to be subtracted:

$$\Delta \theta_{out} = 1.78045 \cdot 10^{-3} - 0.655 \cdot 1.61086 \cdot 10^{-3} = 7.253 \cdot 10^{-4}$$

This result coincides well with the predicted one and confirms that the predominant factors for the limiting radius resolution are angular straggling and the angular resolution of MWPC1/2.

## 7 Scalability of the field

Using the sweep runs (39-61) with different GLAD currents, the scalability of the B-Field can be analyzed. In figure 12  $B_{\rho}$  from GLAD calculator divided by the mean radius is



plotted against the according current values.

Taking the assumption that:

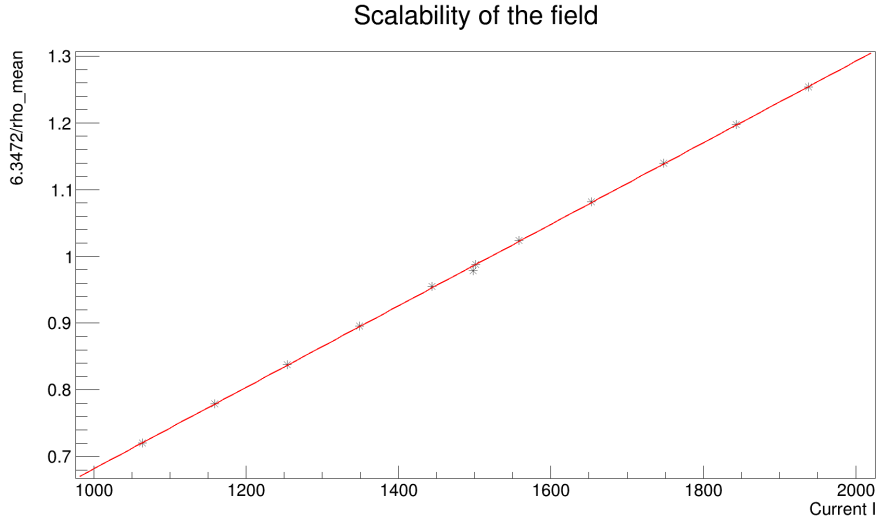


Figure 12

$B = current \cdot k$  (with  $k$  being a constant)

we get from the fit in 12:

slope = 0.000610713

offset = 0.0709244

When plotting the proportional factor  $k$  (which is equal to  $\frac{Brho}{I\rho}$ , with  $Brho$  from GLAD calculator and  $\rho$  equal to the mean radius for each run) for each RUN versus the current and adding the proportional factor from the fit as a straight line, we can see in figure 13 that the factor  $k$  from the fit seems to be slightly underestimated.

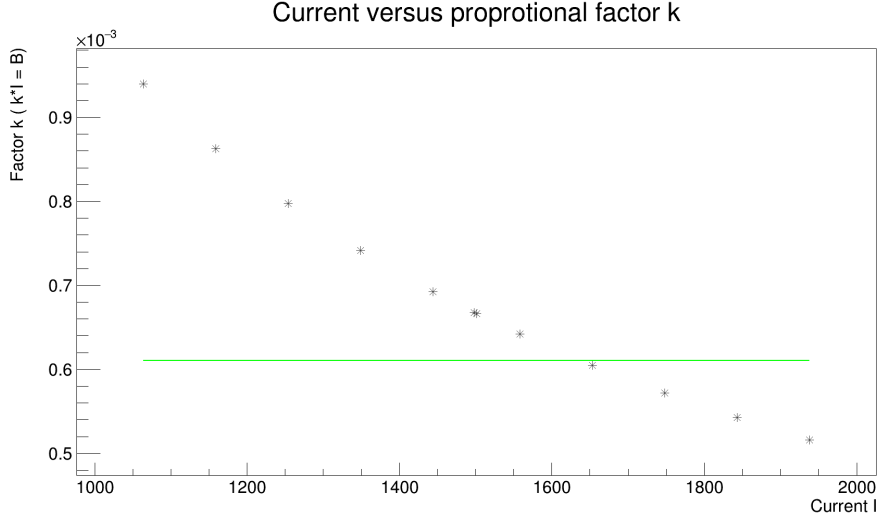


Figure 13

## 8 Z versus A/q calculations

In this section the target RUNs 82,83,86,88 are analyzed with GLAD current = 1444 A, target = CH2 12.29 mm.

Data is taken for the x-position on MW1,MW2 and MW3, time difference between START and TOFW Detector and charge value from TWIM Music.

The radius of curvature in GLAD is computed using the "Advanced Fit Track" method. The time of flight is calculated using the time difference between START and TOFW with the respective offsets (for the TOF detector pads) and subtracting from that the time of flight between START detector and target. The latter is calculated using  $\beta = 0.714549 (\equiv 400 \text{ A/MeV})$  and as distance between START and target 1183.25 mm.

Offsets used for RUNs 82 and 83 ( using sweep RUNs 39-61) and for RUNs 86 and 88 (using sweep run 36), respectively:

Detnr. TOFW	Time offset 39-61 [s]	Time offset 36 [s]	Difference [s]
1	1.15079E-07	1.141E-07	-9.789E-10
2	1.13720E-07	1.13329E-07	-3.910E-10
3	1.16304E-07	1.15778E-07	-5.259E-10
4	1.14539E-07	1.13983E-07	-5.560E-10
5	1.15420E-07	1.14922E-07	-4.979E-10
6	1.16052E-07	1.15593E-07	-4.590E-10
7	1.16903E-07	1.16486E-07	-4.169E-10
8	1.16143E-07	1.15781E-07	-3.620E-10
9	1.14394E-07	1.14067E-07	-3.270E-10
10	1.15967E-07	1.15691E-07	-2.759E-10
11	1.12559E-07	1.12337E-07	-2.220E-10
12	1.15962E-07	1.15764E-07	-1.979E-10
13	1.13521E-07	1.13372E-07	-1.489E-10
14	1.15088E-07	1.14989E-07	-9.900E-11
15	1.13676E-07	1.18635E-07	4.958E-09
16	1.12992E-07	1.17986E-07	4.993E-09
17	1.14391E-07	1.19424E-07	5.033E-09
18	1.12076E-07	1.17168E-07	5.091E-09
19	1.13234E-07	1.18360E-07	5.126E-09
20	1.12760E-07	1.17933E-07	5.173E-09
21	1.16445E-07	1.21687E-07	5.242E-09
22	1.16877E-07	1.22138E-07	5.261E-09
23	1.16077E-07	1.21353E-07	5.275E-09
24	1.16127E-07	1.21457E-07	5.329E-09
25	1.14855E-07	1.20219E-07	5.363E-09
26	1.14363E-07	1.19841E-07	5.477E-09
27	1.14435E-07	1.19932E-07	5.496E-09

The proceeding for the Z versus A/q calculations are:

1. Plot without any cuts/restrictions Z versus Radius using the "Fit-Track" method (see [14](#) ).
2. From that plot identify the various isotopes and cut on them.
3. Plot for each isotope theta\_out vs x\_3 and make a linear fit (see [17](#)).
4. Feed the "Advanced Fit-Track" method with the parameters of the fit for the various isotopes (which you can separate using the previously selected cuts).
5. Calculate beta (using the above TOFW offsets) for the various isotopes and plot Z versus A/q.

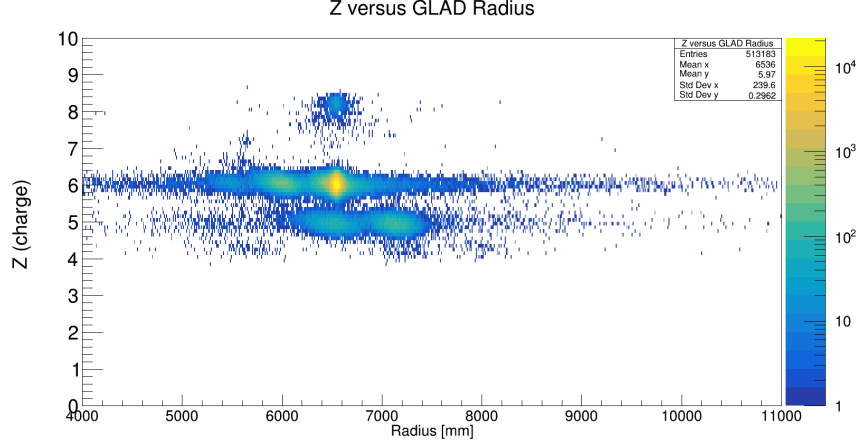
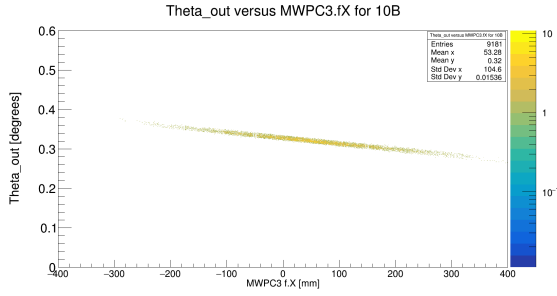
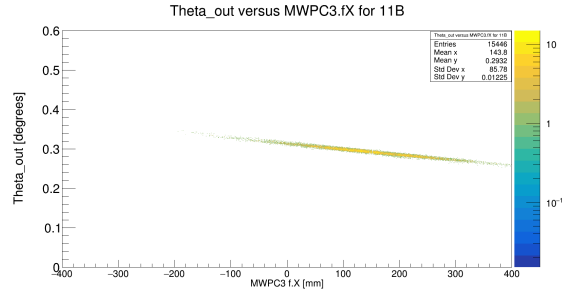


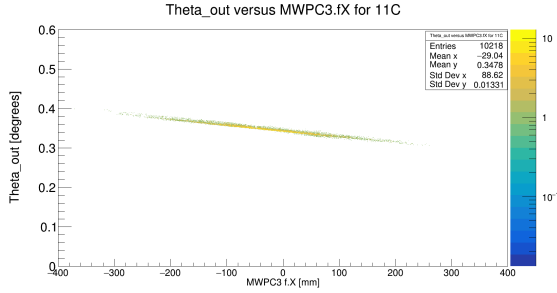
Figure 14: Z versus Radius for RUN 88.



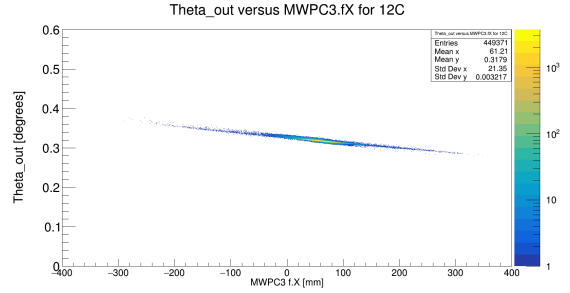
(a) theta\_out vs xMW3 for 10B.



(b) theta\_out vs xMW3 for 11B.



(c) theta\_out vs xMW3 for 11C.



(d) theta\_out vs xMW3 for 12C.

Figure 15: theta\_out vs xMW3 for isotopes.

The cuts on the various isotopes in 14 are:

10B:  $4 < Z < 5.4$  and  $6266 < \rho < 6735$

11B:  $4 < Z < 5.5$  and  $6888 < \rho < 7363$

11C:  $5.2 < Z < 6.8$  and  $5774 < \rho < 6189$

12C:  $5.4 < Z < 6.8$  and  $6295 < \rho < 6768$

Using this cuts we get following fit parameters for the various isotopes:

Isotope	$\alpha$	a (= slope)	b (=offset)
<b>10B:</b>	0.32	0.000144005	0.327681
<b>11B:</b>	0.2932	0.000139928	0.313335
<b>11C:</b>	0.348	0.000146679	0.34352
<b>12C:</b>	0.3179	0.00014353	0.326665

Separating the isotopes by the above charge and radius cuts and using the appropriate  $\alpha$ , a and b parameters the Radius gets recalculated via the "Advanced Fit-Track" method. The new value for the radius is now used in the A/q calculation:

$$A/q = \frac{B \cdot \rho \cdot e}{\gamma \cdot \beta \cdot c \cdot u}$$

with:

$e$ : elementary charge =  $1.602176634 \cdot 10^{-19} \text{C}$

$c$ : speed of light =  $299792458 \text{ m/s}$

$u$ : atomic mass unit =  $1.66053906660 \cdot 10^{-27} \text{kg}$

In figure 16 the separated isotopes are shown.

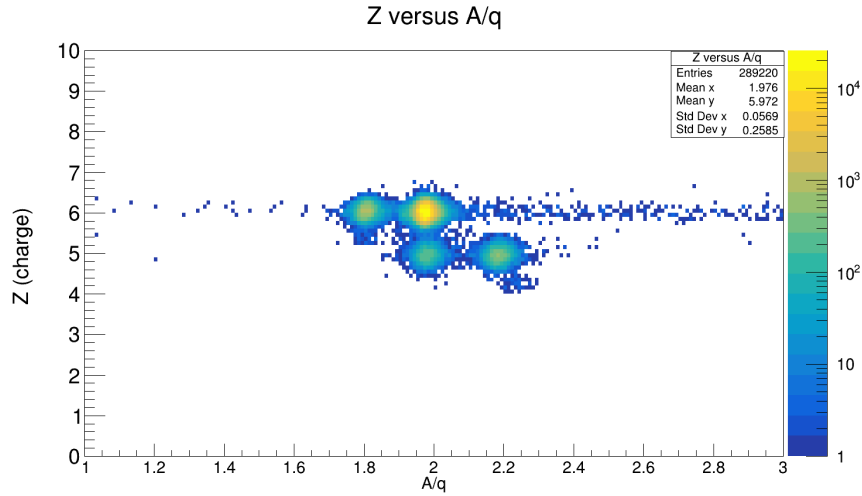


Figure 16: Z versus A/q for run 88 with target CH2 12.29 mm.

## 8.1 Limiting Mass number resolution factors<sup>5</sup>

From the formula:

$$A/q = \frac{B \cdot \rho \cdot e}{\gamma \cdot \beta \cdot c \cdot u}$$

we can see that the determination of A/q is limited by the radius  $\rho$  and time measurement and path calculation .

That means:

---

<sup>5</sup>This analysis was done with RUN 88, CH2 target, 12.29mm, GLAD current = 1444 A on the isotope <sup>12</sup>C

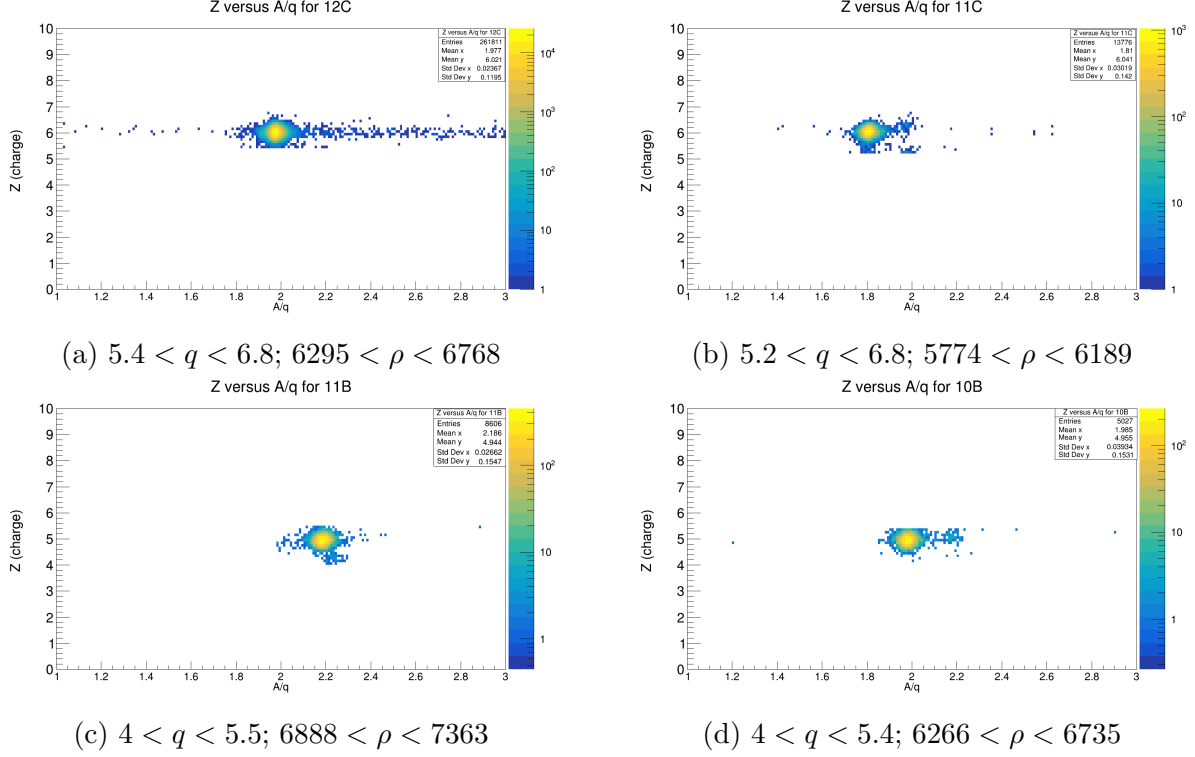


Figure 17: Z versus A/q for runs 82, 83, 86, 88 with target CH2 12.29 mm.

$$\left| \frac{\Delta A/q}{A/q} \right| = \sqrt{\left| \frac{\Delta A/q_\rho}{A/q} \right|^2 + \left| \frac{\Delta A/q_t}{A/q} \right|^2 + \left| \frac{\Delta A/q_s}{A/q} \right|^2}$$

with:

$$\left| \frac{\Delta A/q_\rho}{A/q} \right| = \left| \frac{\Delta \rho}{\rho} \right|$$

and

$$\left| \frac{\Delta A/q_t}{A/q} \right| = \frac{\Delta t}{t \cdot (1 - \beta^2)} \quad 6$$

$\Delta t$  corresponds to the resolution of the time measurement of the TOFW.

As we do not just measure the time of flight in the presence of the magnetic field of GLAD, but the entire flightpath, we use for  $t$  the time of flight from target to the ToFW and as  $s$  the calculated pathlength.

$$t = \frac{s}{\beta \cdot c} = \frac{7.547m}{0.714549 \cdot c} = 3.54 \cdot 10^{-8} s$$

with 7.547m being the mean pathlength for 12C.

When fitting the time of flight we get a resolution of  $\sigma_t = 9.204 \cdot 10^{-2} ns$

From that follows a relative error due to the time resolution:

$$\left| \frac{\Delta A/q_t}{A/q} \right| = \frac{9.12 \cdot 10^{-11}}{3.54 \cdot 10^{-8} (1 - 0.714549^2)} = 5.31 \cdot 10^{-3}$$

From fit we get for  $\left| \frac{\Delta A/q_\rho}{A/q} \right| = \frac{11.91}{6554.7} = 1.82 \cdot 10^{-3}$  with 11.91 being the  $\sigma_\rho$  and 6554.7 the

$${}^6 d\beta = -\frac{s}{c \cdot t^2} \Delta t = -\frac{\beta \cdot \Delta t}{t}; \quad \frac{dA/q}{d\beta} = -B \cdot \rho \cdot \frac{1}{\beta^2 \cdot \sqrt{1 - \beta^2}} \Delta \beta = \frac{B \cdot \rho}{\beta \cdot t \cdot \sqrt{1 - \beta^2}} \cdot \Delta t$$

$\rho_{mean}$  values in mm.

$\left| \frac{\Delta A/q_s}{A/q} \right| = \frac{\Delta s}{s \cdot \sqrt{1-\beta^2}}$  As main source of error for the pathlength it is assumed to be the reconstruction of the radius and therefore the main source of error is  $\rho \cdot \omega$  which is about 2.09m. From that we calculate:  $\Delta s = \frac{2.09}{6.5547} \cdot \sigma_\rho = 3.798mm$

Hence:

$$\left| \frac{\Delta A/q_s}{A/q} \right| = 1.03 \cdot 10^{-3}$$

Summing up all errors quadratically we get:

$$\left| \frac{\Delta A/q}{A/q} \right| = \sqrt{(5.31 \cdot 10^{-3})^2 + (1.82 \cdot 10^{-3})^2 + (1.03 \cdot 10^{-3})^2} = 5.7 \cdot 10^{-3}$$

From the fit of the data plot Z vs. A/q we get:

$$\left| \frac{\Delta A/q}{A/q} \right| = \frac{\sigma_{A/q}}{A/q_{mean}} = 1.25 \cdot 10^{-2} / 1.976 = 6.73 \cdot 10^{-3}$$

As we see the estimated resolution factor is slightly smaller than the one from the data fit. It could be that the resolution factor for the pathlength was underestimated or that these small deviations come from binning effects.

### 8.1.1 Z vs A/q resolution for all isotopes - summary

## 8.2 Z versus A/q calculations with (fixed) $\beta$

In the previous section I used both reconstructed pathlength and time of flight from data to compute the  $\beta$  value for each event. In this section I use a fixed  $\beta = 0.714549$  (i.e. 400A/MeV) to calculate A/q. This simplifies the error calculation:

$$\left| \frac{\Delta A/q}{A/q} \right| = \left| \frac{\Delta \rho}{\rho} \right|$$

That means the relative resolution of A/q should be the same as for  $\rho$ .

From the plots we get follwing resolutions for A/q and for  $\rho$  (for RUN 88):

Isotope	A/q	$\left  \frac{\Delta A/q}{A/q} \right $	A/q (fixed $\beta$ )	$\left  \frac{\Delta A/q}{A/q} \right $ (fixed $\beta$ )	$\left  \frac{\Delta \rho}{\rho} \right $
<b>10B:</b>	1.981	1.036E-02	1.937	8.606E-03	8.679E-03
<b>11B:</b>	2.186	9.904E-03	2.112	7.102E-03	7.061E-03
<b>11C:</b>	1.807	9.753E-03	1.786	7.519E-03	7.514E-03
<b>12C:</b>	1.977	6.731E-03	1.947	1.874E-03	1.835E-03

As expected  $\left| \frac{\Delta A/q}{A/q} \right|$  (for fixed  $\beta$ ) and  $\left| \frac{\Delta \rho}{\rho} \right|$  are almost equal in value. Small deviations are likely credited to binning effects (rel. bin-width for  $\left| \frac{\Delta A/q}{A/q} \right|$  calculation is  $\approx 5 \cdot 10^{-2}$ , for  $\left| \frac{\Delta \rho}{\rho} \right| \approx 8 \cdot 10^{-4}$ ).

### 8.2.1 Time of Flight versus $A/q$

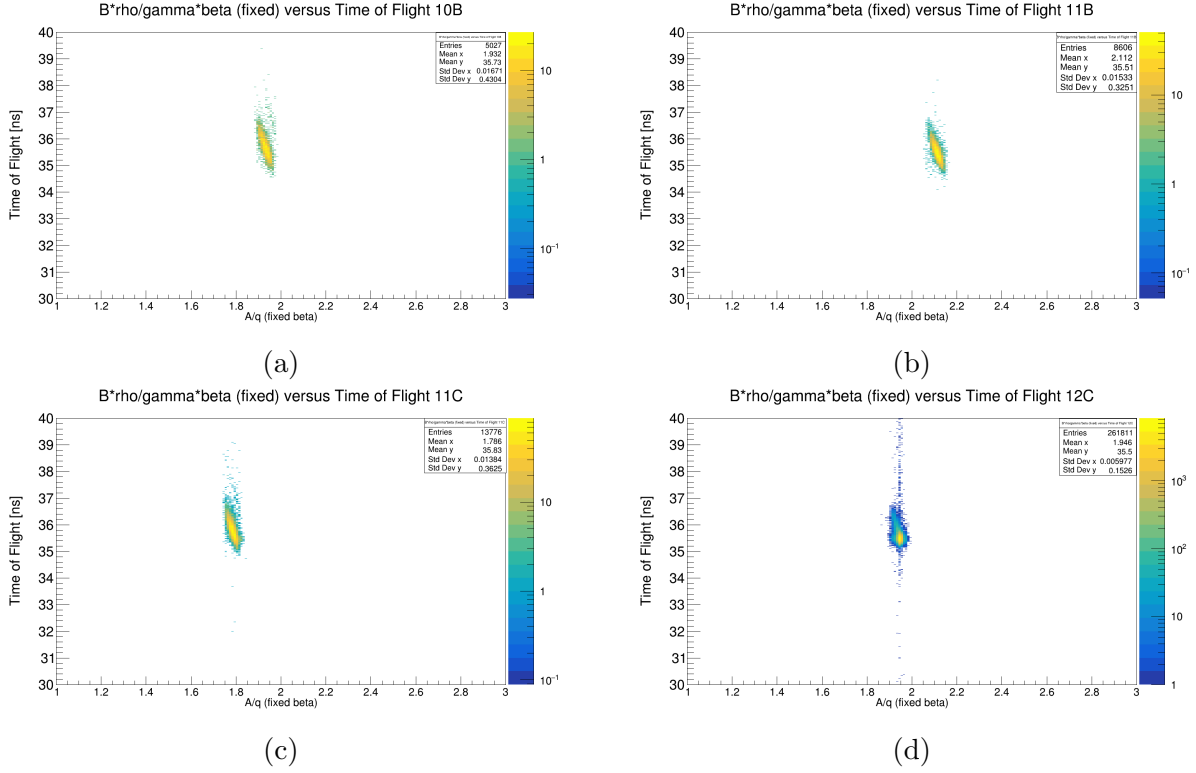


Figure 18: Time of Flight versus  $A/q$  with fixed  $\beta$  for RUN 88.

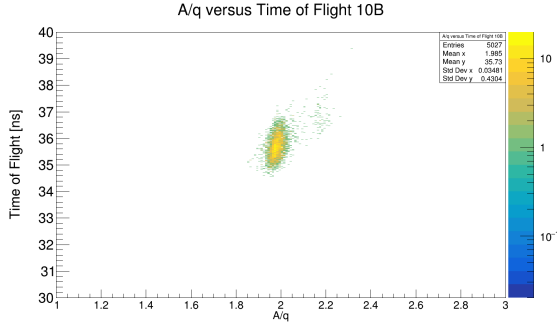
When looking at the formula:

$$A/q = \frac{B \cdot \rho \cdot e}{\gamma \cdot \beta \cdot c \cdot u}$$

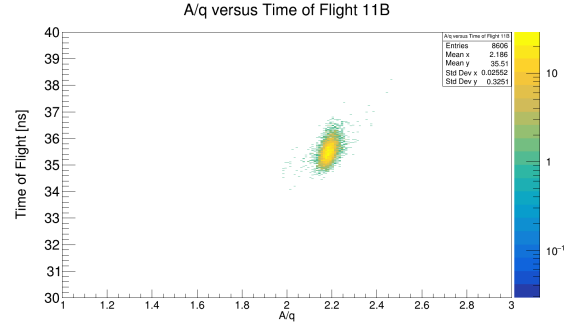
we can reconstruct that if setting  $\gamma$  and  $\beta$  as fixed values  $A/q$  will increase for isotopes with high velocity (short time of flight) and vice versa. Figure 18 reflects this behavior.

Using instead the time of flight and the reconstructed pathlength for each event for the calculation of  $\gamma$  and  $\beta$  in the  $A/q$  calculation it is expected to vertically straighten the plots. This is the case, see figure 19. But the plots smear out a lot ( $|\frac{\Delta A/q_t}{A/q}|$  is the major source of error. This was already shown in previous sections). Hence the calculation of  $A/q$  with fixed  $\beta$  (and  $\gamma$ ) is preferred.

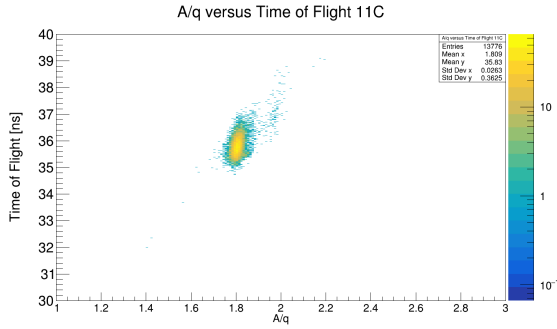




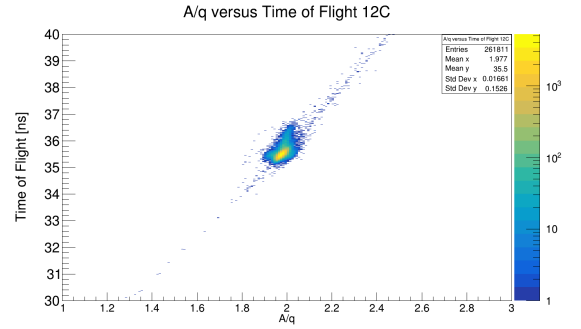
(a)



(b)



(c)



(d)

Figure 19: Time of Flight versus  $A/q$  with  $\beta$  from time measurement and flightpath reconstruction for RUN 88.

# Appendices

## A Radius resolution with minimal constraints

When using minimal constraints (one single fX entry in MWPC0,1,2,3; instead of requiring also one single entry in fY for MW0,1,2,3) for events in sweep RUN 39-61 the resolution for the radius determination improves:

Runnr.	$\bar{\rho}$	$\sigma$	rel. resolution
39	6.48993e+03	2.30085e+01	3.545e-03
40	6.42478e+03	1.23238e+01	1.918e-03
42	6.20135e+03	1.16977e+01	1.886e-03
44	5.86911e+03	1.05839e+01	1.803e-03
46	5.57055e+03	9.45711e+00	1.697e-03
48	5.30096e+03	8.63127e+00	1.628e-03
51	5.06178e+03	8.99078e+00	1.776e-03
53	6.64685e+03	1.30785e+01	1.967e-03
55	7.08715e+03	1.56974e+01	2.214e-03
57	7.57535e+03	1.68392e+01	2.222e-03
59	8.15170e+03	1.93779e+01	2.377e-03
61	8.81023e+03	2.33200e+01	2.646e-03

With the exception of RUN 39 (why??) the resolution improve with low constraints. This could be due to the lower angular straggling impact when particles don't hit/interact with the y-wires of the MWPCs.

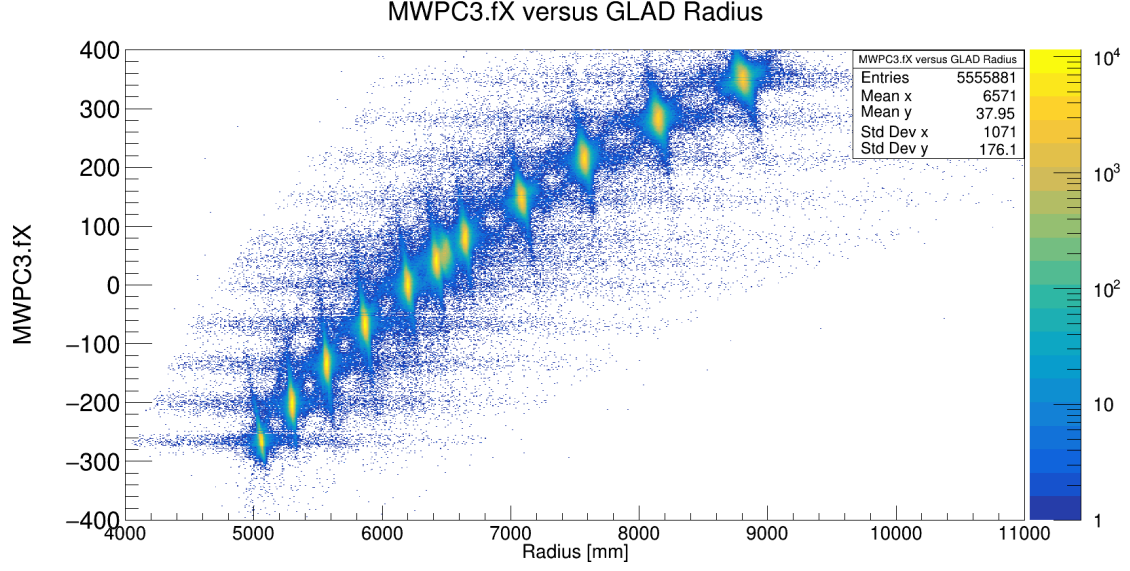


Figure 20: MW3.fX vs GLAD Radius for RUNs 39-61 with low constraints.

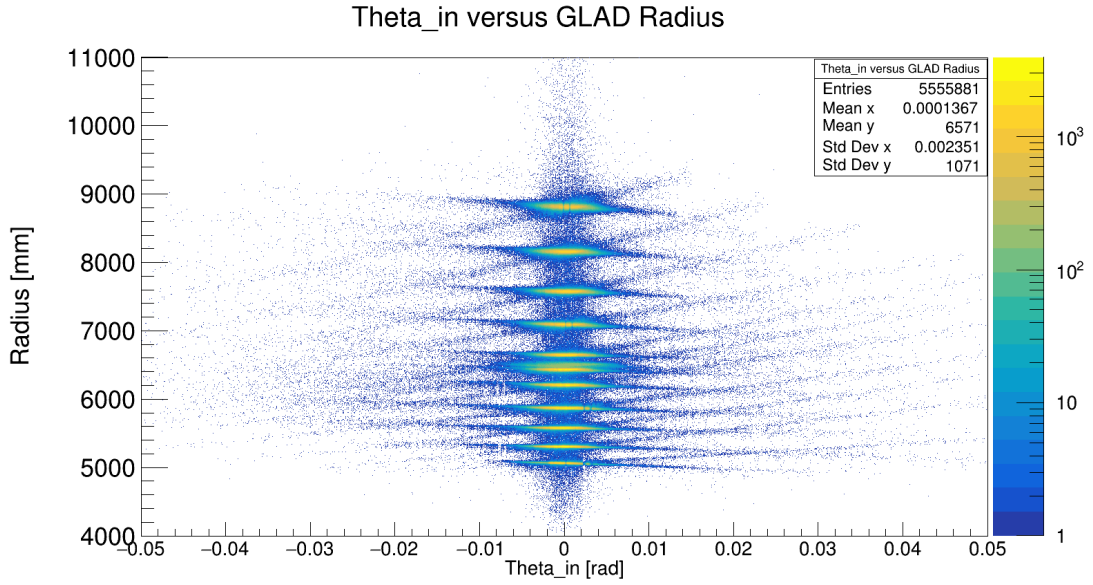


Figure 21: Theta\_in vs GLAD Radius for RUNs 39-61 with low constraints.

## B Time of Flight Calibration

To make the Time of Flight(ToF) calibration, two methods were used:

1. Calculate the ToF resolution =  $\text{pathlength}(\text{for plastic}) / (\text{velocity})$  where the pathlength is a fixed parameter for each plastic while velocity =  $\text{pathlength} / \text{calibrated time of}$

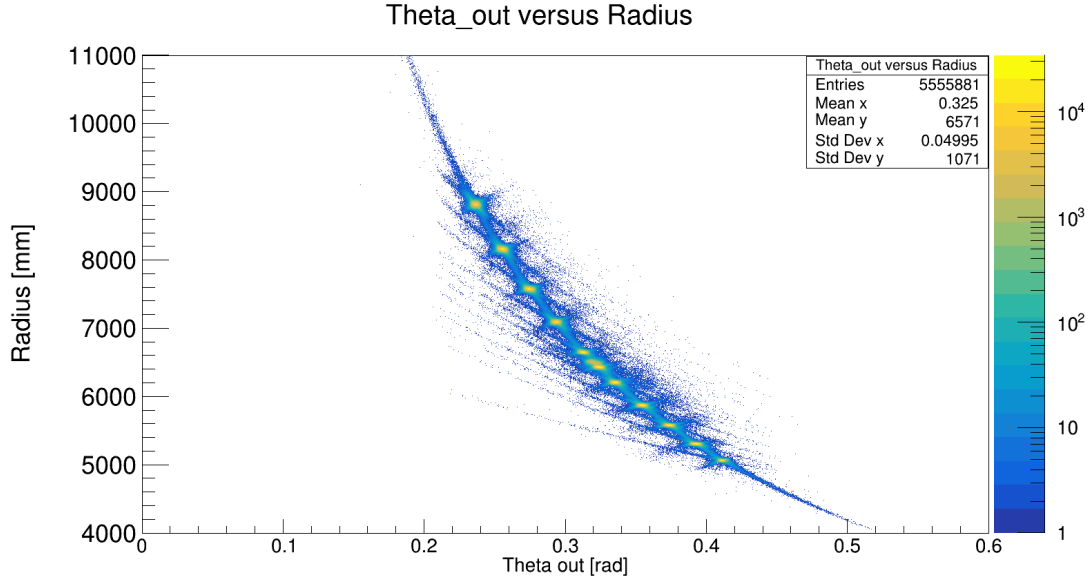


Figure 22: Theta\_out vs GLAD Radius for RUNs 39-61 with low constraints.

flight (for each event).

2. To remove events with large deviations in the y direction in MWPC3 a cut was made on MWPC3.fY:  $-20 < f.Y < 20$  (mm)  
Using the first method we get following ToF resolutions:

Detectornr. TOFW	mean ToF [ <i>ns</i> ]	Std_dev [ <i>ns</i> ]
1	4.64761e+01	3.81923e-01
2	4.64675e+01	3.67167e-01
3	4.63957e+01	7.76052e-02
4	4.63900e+01	6.73563e-02
5	4.63862e+01	1.00703e-01
6	4.63625e+01	6.97601e-02
7	4.63563e+01	7.85820e-02
8	4.63437e+01	8.22121e-02
9	4.63391e+01	8.67345e-02
10	4.63271e+01	1.57514e-01
11	4.63336e+01	1.34324e-01
12	4.63184e+01	1.16769e-01
13	4.63244e+01	1.04881e-01
14	4.63157e+01	9.15921e-02
15	4.63137e+01	8.36279e-02
16	4.63184e+01	9.34706e-02
17	4.63183e+01	9.16414e-02
18	4.63281e+01	1.60578e-01
19	4.63294e+01	1.06840e-01
20	4.63203e+01	1.19530e-01
21	4.63625e+01	5.28339e-01
22	4.63434e+01	9.61574e-02
23	4.63285e+01	1.00733e-01
24	4.63771e+01	1.43214e-01
25	4.63691e+01	9.87333e-02
26	4.63947e+01	3.17881e-01
27	4.63994e+01	7.93419e-02

Using the second methods with strict constraints on MWPC3.fY we get:

Detector number (TOFW)	Meanval [ <i>ns</i> ]	Std_dev [ <i>ns</i> ]	No. of Events
1	46.61	0	1
2	4.64900e+01	1.43336e-01	22
3	4.65016e+01	7.35427e-02	1402
4	4.65008e+01	7.16455e-02	925
5	4.64769e+01	9.06103e-02	190
6	4.64772e+01	6.89027e-02	2536
7	4.64662e+01	7.08772e-02	264
8	4.64608e+01	8.49612e-02	879
9	4.64600e+01	8.13301e-02	1744
10	4.64793e+01	1.59559e-01	84
11	4.64527e+01	1.38096e-01	1920
12	4.64527e+01	1.24507e-01	563
13	4.64487e+01	7.71276e-02	505
14	4.64596e+01	1.00582e-01	2536
15	4.64662e+01	7.93961e-02	3034
16	4.64687e+01	8.62515e-02	1500
17	4.64790e+01	8.80871e-02	2988
18	4.64777e+01	1.13045e-01	164
19	4.65012e+01	9.91565e-02	1845
20	4.64933e+01	1.16504e-01	1696
21	4.64629e+01	4.95801e-01	183
22	4.65383e+01	9.55104e-02	2840
23	4.65253e+01	1.16294e-01	352
24	4.65977e+01	1.82543e-01	868
25	4.65789e+01	1.09101e-01	2235
26	4.65862e+01	1.88742e-01	65
27	4.66393e+01	7.99918e-02	1739

From the second method we get a mean value for the std\_dev. of 0.121 ns (neglecting the std\_dev. for Detnr. 1, as we just have one event there).

Without Detnr. 21, which doesn't have a good resolution, we get a mean std\_dev. of 0.105 ns.